

# A Multilevel Turbo-Code with Antenna Diversity

Dongzhe Cui, Alexander M. Haimovich and Hangjun Chen  
CCSPR Lab, Dept. of Electrical and Computer Engineering  
New Jersey Institute of Technology  
Newark, New Jersey 07102, USA

e-mail: dxc1207@njit.edu, haimovic@njit.edu, hxc1170@njit.edu

*Abstract*— A channel coding scheme is analyzed that features parallel concatenated systematic space-time codes with multilevel modulation and multiple transmit/receive antennas. The proposed scheme is referred to as *turbo space-time coded modulation* (turbo-STCM). It combines the advantages of powerful turbo codes with the diversity of space-time coded modulation. The scheme utilizes recursive and systematic constituent space-time codes and features full diversity and full rate. Simulation results are provided for 8-PSK schemes over the block-fading channel. It is shown that this turbo scheme provides an advantage of 1.1 dB over conventional space-time codes of similar decoding complexity. The analytical union bound of the bit error probability is derived for turbo-STCM over the Rayleigh block-fading channel. The bound makes it possible to express the performance analysis of turbo-STCM in terms of the properties of the constituent space-time codes. The union bound is demonstrated for 8-PSK turbo-STCM with two transmit antennas and one/two receive antennas.

## I. INTRODUCTION

Turbo-code [1] when combined with iterative decoding have been shown to provide excellent coding gains. Like turbo code, space-time code (STC) is a newly invented family of codes. Diversity advantage of space-time processing is combined with the bandwidth efficiency and error correction coding of trellis coded modulation [2]. It is natural to expect that merging turbo-coding and space-time code could lead to the design of better codes for the fading channel. Recently, several schemes that combine turbo and space-time codes were proposed. Serially concatenated space-time codes and turbo-codes were proposed in [3]. A serial concatenation of space-time codes and recursive convolutional codes was presented in [4]. A different serial concatenation as well as a parallel concatenation scheme were shown in [5]. In [6], the outputs of binary turbo-codes were mapped to QPSK symbols and transmitted through multiple antennas. A scheme that maps the outputs of recursive convolutional encoders to different antennas was proposed in [7]. Another parallel concatenation with the outputs of recursive encoders mapped to different antennas was presented in [8]. Some of these schemes provide full space diversity and full coding rate.

A different approach is obtained by evolving from turbo-codes to trellis coded modulated turbo-codes [9]. Extending this idea, we proposed a scheme that parallel concatenate of two systematic space-time code modules [10], [11], [12]. We referred to this scheme as turbo space-time

coded modulation (turbo-STCM). It utilizes the principle of iterative processing directly to the STC modules. The output signals are punctured resulting in a full rate code. This scheme can be viewed as a true extension of the original turbo scheme [1] from the bit to the symbol level. An iterative symbol-by-symbol *maximum a posteriori* algorithm operating in the log domain is developed for decoding turbo-STCM [10]. In [11], we developed the upper bound for turbo-STCM with two transmit antenna over the additive white Gaussian noise (AWGN) channel. In this paper, we extend it to the block-fading channel.

The paper is organized as follows. In the section II, we briefly present the system model and iterative decoding algorithm. Section III shows numerical simulations and comparisons with other methods for 3 bits/s/Hz turbo-STCM codes utilizing 8-PSK modulation. Section IV contains the theoretical performance analysis of turbo STCM. Numerical examples including simulations are found in section V. Finally, conclusion are presented in section VI.

## II. SYSTEM MODEL

The goal of turbo-STCM is to apply the turbo structure to space-time code. The turbo-STCM encoder consists of two systematic STC modules operating in a parallel concatenation structure. The systematic recursive 16 state 8-PSK STC is shown in Fig. 1. Systematic component codes are often encountered in turbo-codes applications due to their good performance at low signal-to-noise ratios. The systematic structure is further motivated by the need to puncture the parity data of the turbo code such the data rate of the overall code is the same as that of the constituent codes. A block diagram of the turbo-STCM encoder with two transmit antennas is shown in Fig. 2. Details of turbo-STCM encoding operation can be found in [10], [11].

A schematic diagram of the transmission system is shown in Fig. 3. The architecture of a turbo-STCM encoder with  $N = 2$  transmit antennas is shown in Fig. 2. Let a source generate an information bit sequence  $u$ . Using  $k$  to denote the time index, turbo-STCM encodes the information bits  $u_k$  to  $N$  symbols represented by the binary column vectors  $\mathbf{c}_k^{(n)}$ ,  $n = 1, \dots, N$ . Those are fed into a memoryless mapper  $\rho(\cdot)$  that emits the symbols  $s_k^{(n)} = \rho(\mathbf{c}_k^{(n)})$ . In this paper,  $s_k^{(n)}$  are 8-PSK symbols.

Define the symbol vector  $\mathbf{s}_k \in \mathcal{C}^N$ ,  $\mathbf{s}_k = \left[ s_k^{(1)} \dots s_k^{(N)} \right]^T$ ,

where the superscript denotes transposition. For a turbo-STCM receiver utilizing an array of  $M$  antennas, the channel output symbols are represented by  $M \times 1$  vectors  $\mathbf{y}_k \in \mathcal{C}^M$  are

$$\mathbf{y}_k = \sqrt{E_s} \mathbf{H} \mathbf{s}_k + \mathbf{z}_k, \quad (1)$$

where  $E_s$  is the energy per symbol, related to the energy per bit by  $E_s = mE_b$  ( $m = 3$  in this paper). The  $M \times N$  matrix  $\mathbf{H}$  consists of the channel coefficients. The channel is assumed flat, Rayleigh and block-fading. Additive white Gaussian noise is modeled by the vector  $\mathbf{z}_k$ . The noise is assumed complex-valued, Gaussian distributed with zero-mean and variance  $N_0/2$  for each dimension.

As in [10], [11], [13], turbo-STCM decoder is an iterative processing structure as shown in Fig. 4. The decoder employs two *a posteriori* probability (APP) computing modules concatenated in parallel; one module for each constituent code. These decoders are denoted in Fig. 4, APP1 and APP2, respectively. The generic APP algorithm for nonbinary trellis and multiple-input-multiple-output channel is based on the BCJR algorithm [14] and on [9]. The multiplicative form of the APP algorithm can be converted into an additive form by converting to the log domain. For an hypothesis information symbol  $u_k = u^{(i)}$  and given the sequence of observations  $\mathbf{Y}$ , the soft output of the log-APP at time  $k$  is:

$$M(u_k = u^{(i)} | \mathbf{Y}) = \Psi(\mathbf{y}_k | u^{(i)}) + L(u_k = u^{(i)}), \quad (2)$$

where  $M(u_k = u^{(i)} | \mathbf{Y}) = \log P(u_k = u^{(i)} | \mathbf{Y})$  is the log-APP,  $\Psi(\mathbf{y}_k | u^{(i)})$  incorporates the systematic and extrinsic information, and  $L(u_k = u^{(i)}) = \log P(u_k = u^{(i)})$  is the a priori information. The a priori input to each APP decoder can be derived from the output of the *other* decoder. Data is shared between the two decoders, and an iterative process is applied to refine the soft decisions.

### III. NUMERICAL RESULTS

We present simulation results on the performance of our turbo-STCM scheme for 3 bits/s/Hz 8-PSK. The channel model was Rayleigh block-fading, meaning that the channel was assumed constant during a frame of  $F = 130$  symbols, but independent frame-to-frame. Two types of interleavers were used in the simulations. With the first type, each sequence of size  $K$  symbols was run with a different random interleaver chosen from a uniform distribution. Performance shown for random interleavers is the average over all interleavers. In the figures, curves representing performance averaged over uniform random interleavers are labeled ‘UIL’. The second type of interleaver used in the simulations was an ‘S-random’ interleaver, as suggested in [15]. Following guidelines in the reference and choosing  $S = 25$ , an interleaver was obtained by generating random permutations (interleaves) without replacement, subject to the restriction that adjacent symbols are not interleaved within a distance of  $S$  symbols of each other. This interleaver was used in all simulations with fixed interleaver and the curves were labeled ‘FIL’. For brevity of notation and for easier correlation with the

figures, we use the ‘UIL’ and ‘FIL’ designations in the description below. Figure captions specify the number of transmit-receive antenna, e.g., 2T1R = two transmit-one receive antenna. Individual codes are labeled according to the modulation and number of states (“8p16s” refers to 8-PSK modulation, 16 state code).

Fig. 5 shows the frame error rate (FER) for two transmit-one receive antenna 2 bits/s/Hz turbo-STCM,  $K = 1300$  symbols interleaver and with recursive systematic terminated constituent codes. As we know, although it is possible to terminate the trellis of either constituent encoder with the tail bits, the simultaneous termination of both trellises is almost impossible due to the interleaver and the recursive structure which makes it much difficult to compute the tail bits [16, Page. 38]. In Fig. 5, we solve the problem by terminating one of recursive systematic upper code and leaving another one “open”. The only modification of the MAP decoding algorithm is that the backward recursion computation needs to be initialized as that either state can be the end of trellis [16, Page. 65]. Performance is shown for fixed interleaver ‘FIL’ after 1, 4, and 8 iterations. Curves are also provided for 64 state 4-PSK Tarokh *et al.* codes [2]. It is observed that after 4 iterations at FER=10<sup>-2</sup>, turbo-STCM has an advantage of 3.7 dB over Tarokh’s 64 state code. This advantage becomes 4.5 dB after 8 iterations.

Fig. 6 shows the frame error rate (FER) for two transmit-one receive antenna turbo-STCM,  $K = 1300$  symbols interleaver and with recursive systematic 16 state 8-PSK constituent codes as shown in Fig. 1. Performance is shown for the fixed interleaver (FIL) after 8 iterations after 3, and 8 iterations. Curves are also provided for two transmit-one receive antenna 8-PSK 16 state and 64 state Tarokh *et al.* codes [2]. Finally, the performance of our designed recursive and systematic space-time constituent code is also shown. It is observed that at high  $E_b/N_0$ , all codes provide full diversity as demonstrated by the parallel asymptotic slopes. In particular, our systematic recursive code has the same diversity as Tarokh’s code (same slope) but lower coding gain (approximately 1.5 dB at FER = 10<sup>-1</sup> compared to Tarokh’s 16 state code). However, after 3 iterations, turbo-STCM with fixed interleaver has an advantage of 2 dB over Tarokh’s 16 state code at FER = 10<sup>-1</sup>. This advantage becomes 3.4 dB after 8 iterations. The 64 state Tarokh code is shown since it has roughly the same decoding complexity as turbo-STCM with 16 state constituent codes, 3 iterations and two APP decoders per iteration. At FER = 10<sup>-1</sup>, turbo-STCM with fixed interleaver (FIL) has about 1.1 dB advantage after 3 iterations over a stand-alone space-time code of comparable complexity. This advantage becomes 2.3 dB after 8 iterations.

Fig. 7 is similar to Fig. 6, except that two antennas are used at the receiver. The approximately parallel slopes of all curves indicate that all methods shown provide full diversity. In this case, the advantage of turbo-STCM with fixed interleaver after 8 iterations over Tarokh code with 64 states is only about 1 dB (at FER = 10<sup>-2</sup>).

Fig. 8 shows the FER comparison of turbo-STCM with recursive and non-recursive STC, fixed interleaver (FIL) and averaged over interleavers (UIL). The non-recursive STC is described detail in [17]. In 2T1R case, approximately 1 dB advantage of the fixed interleaver (FIL) is over the averaged random interleaver (UIL) after 8 iterations at FER=10<sup>-2</sup> while 1.3 dB advantage of recursive component STC is over non-recursive component STC. 2T2R is similar to 2T1R, except that the advantage of turbo-STCM with ‘FIL’ over ‘UIL’ is 0.5 dB.

#### IV. TURBO-STCM PERFORMANCE ANALYSIS

In this section, the interleaver is assumed random with uniform distribution (UIL). Then the performance bound analysis is carried out by averaging over the interleavers. we revisit definitions and notations used for the union bound for the AWGN channel and introduced in [11], [13]. Subsequently, we proceed to develop the union bound for the fading channel. The specific STC example is considered for 8-PSK, 16-state. To derive the bound, we first classify the error sequences into different types from the point of view of error event probability. That takes into account all possible transmitted and received codewords in computing the union bound. Due to the uniform random interleaver, all the error sequences of the same error type have the same occurrence probability, while different error types have different occurrence probability. The computation of the union bound proceeds by finding the average number of error sequences in each type together with their probability. Finally, we compute the union bound by averaging all squared Euclidean distances of each error type and averaging over the fading channel realizations.

The output of the turbo-STCM code consists of the sum of the systematic part and punctured parity part. Given a systematic block code  $\mathbf{c}$  of length  $K$  symbols, the set of transmitted codewords and received codewords, the function  $a(6K, w, z)$  denotes the number of *error* sequences of length  $6K$  bits that have Hamming weight  $w$  for the information bits and  $z$  for the parity bits. We refer to such error sequences as  $(w, z)$  sequences. The overall Hamming weight of these sequences is  $w + z$ . A method for computing the input-output weight enumerator (IOWE) coefficients  $a(6K, w, z)$  for punctured STC is given in [11]. Here we assume that these coefficients are available. It is also shown that given the coefficients of the constituent STC codes, say  $a_1(6K, w, z_1)$  and  $a_2(6K, w, z_2)$ , the turbo-STCM coefficients can be found from

$$\tilde{a}(6K, w, z) = \sum_{z_1+z_2=z} \frac{a_1(6K, w, z_1)a_2(6K, w, z_2)}{\binom{3K}{w}}, \quad (3)$$

where  $0 \leq w \leq 3K$  and  $0 \leq z \leq 3K$ . This expression is used to evaluate the IOWE’s of turbo-STCM given the IOWE’s of the constituent codes.

2<sup>m</sup>-PSK turbo-STCM accepts  $m$  ( $m=3$  here) binary symbols at a time and transforms them into  $N$  (number of transmit antenna) blocks of binary symbols that are fed

into a memoryless mapper  $\rho(\cdot)$ . The noiseless received symbol is,

$$f(\mathbf{c}_k) = h_1 s_k^1 + h_2 s_k^2 = \mathbf{h}^T \rho(\mathbf{c}_k) \quad (4)$$

where  $\mathbf{h}^T = [h_1 h_2]$  is substituted for  $\mathbf{H}$  in signal model (1). Let  $\underline{\mathbf{c}}_K = (\mathbf{c}_1, \dots, \mathbf{c}_K)$  be a sequence of  $K$  binary codewords associated with the  $K$  transmitted symbols. An error event occurs when the demodulation chooses transmitted symbols corresponding to  $\underline{\mathbf{c}}_K \oplus \underline{\mathbf{e}}_K$  and  $\underline{\mathbf{e}}_K$  is a non-zero sequence of binary error vectors.

The pairwise error probability of choosing  $\underline{\mathbf{c}}_K \oplus \underline{\mathbf{e}}_K$  instead of  $\underline{\mathbf{c}}_K$  is denoted  $P(\underline{\mathbf{c}}_K \rightarrow \underline{\mathbf{c}}_K \oplus \underline{\mathbf{e}}_K)$  and is given by

$$\begin{aligned} P(\underline{\mathbf{c}}_K \rightarrow \underline{\mathbf{c}}_K \oplus \underline{\mathbf{e}}_K) &= Q\left(\sqrt{\frac{r_c E_b d^2(\underline{\mathbf{c}}_K, \underline{\mathbf{e}}_K)}{2N_0}}\right) \\ &\leq \frac{1}{2} Z^{d^2(\underline{\mathbf{c}}_K, \underline{\mathbf{e}}_K)}, \end{aligned} \quad (5)$$

where  $Z = e^{-r_c E_b / 4N_0}$ ,  $r_c = m/Nm$  is the turbo-STCM code rate and  $d^2(\underline{\mathbf{c}}_K, \underline{\mathbf{e}}_K) = \|f(\underline{\mathbf{c}}_K) - f(\underline{\mathbf{c}}_K \oplus \underline{\mathbf{e}}_K)\|^2$  is the cumulative squared Euclidean distance (SED) associated with  $\underline{\mathbf{c}}_K$  and  $\underline{\mathbf{e}}_K$ .

The *type* of an error sequence is defined as the vector  $\mathbf{n}$  with elements  $n_{ij}$  denoting the number of symbols in the error sequence that have  $i$  systematic bit errors and  $j$  parity bit errors. For the 3 bits/s/Hz, 8-PSK 2 transmit antennas we have  $(i, j) \in (0,1), (0,2), (0,3), (1,0), (1,1), (1,2), (1,3), (2,0), (2,1), (2,2), (2,3), (3,0), (3,1), (3,2), (3,3)$ . The following relations can be found

$$\begin{aligned} w &= n_{10} + n_{11} + n_{12} + n_{13} + 2n_{20} + 2n_{21} + 2n_{22} \\ &\quad + 2n_{23} + 3n_{30} + 3n_{31} + 3n_{32} + 3n_{33} \\ z &= n_{01} + 2n_{02} + 3n_{03} + n_{11} + 2n_{12} + 3n_{13} + n_{21} \\ &\quad + 2n_{22} + 3n_{23} + n_{31} + 2n_{32} + 3n_{33}. \end{aligned} \quad (6)$$

The mapping  $\mathbf{n} \rightarrow (w, z)$  is many-to-one. Let  $\Phi(w, z, \mathbf{n})$  denote the probability that  $(w, z)$  error sequence is also of type  $\mathbf{n}$ .  $\beta$  is indexed with all types of error sequences  $(w, z)$ , i.e.,  $\bigcup_{\beta} \mathbf{n}_{\beta}(w, z)$  is the set of  $(w, z)$  error sequences. Following [11], the conditional upper bound on the bit error probability is given by

$$\begin{aligned} P(e|\mathbf{h}) &\leq B(e|\mathbf{h}), \\ &= \sum_{w=1}^{3K} \sum_{z=0}^{3K} \sum_{\mathbf{n}_{\beta}(w,z)} \frac{w}{6K} \tilde{a}(6K, w, z) \Phi(w, z, \mathbf{n}_{\beta}) E[Z^{D_{\mathbf{n}_{\beta}}^2}] \quad (7) \end{aligned}$$

where the term  $E[Z^{D_{\mathbf{n}_{\beta}}^2}]$  is the expectation over SED’s associated with error sequences of type  $\mathbf{n}_{\beta}(w, z)$  and the notation  $B(e|\mathbf{h})$  denotes the bound. It follows that the average upper bound to the bit error probability is given by

$$\begin{aligned} B(e) &= E_{\mathbf{h}}[B(e|\mathbf{h})] \\ &= \sum_{w=1}^{3K} \sum_{z=0}^{3K} \sum_{\mathbf{n}_{\beta}(w,z)} \frac{w}{6K} \tilde{a}(6K, w, z) \Phi(w, z, \mathbf{n}_{\beta}) E_D \left\{ E_{\mathbf{h}}[Z^{D_{\mathbf{n}_{\beta}}^2}] \right\} \end{aligned} \quad (8)$$

where we switched the order of the expectation operations with respect to  $D$  and  $\mathbf{h}$ . We now focus on evaluating the term  $E_{\mathbf{h}} \left[ Z^{D_{\mathbf{n}_\beta}^2} \right]$ . The SED for a single epoch of an error path can be expressed

$$d^2(\mathbf{c}_k, \mathbf{e}_k) = \left\| \sum_{n=1}^2 h_n (\rho(c_{n,k}) - \rho(c_{n,k} \oplus e_{n,k})) \right\|^2 \quad (9)$$

Subsequently, the cumulative SED associated with an error sequence can be expressed in terms of the channel:

$$\begin{aligned} d^2(\underline{\mathbf{c}}_K, \underline{\mathbf{e}}_K) &= \sum_{k=1}^K \left\| \sum_{n=1}^2 h_n (\rho(c_{n,k}) - \rho(c_{n,k} \oplus e_{n,k})) \right\|^2 \\ &= \mathbf{x}^H \mathbf{x} \end{aligned} \quad (10)$$

where the superscript  $H$  denotes complex and transposed.  $\mathbf{x}$  is  $K \times 1$  vector and has complex-valued Gaussian multivariate with zero mean and covariance matrix  $\mathbf{M}_{\mathbf{x}} = \text{cov}(\mathbf{x}) = (\mathbf{m}_{ij})$ .

$$(m_{ij}) = \begin{cases} i = j & \sum_{n=1}^2 d^2(c_{n,i}, e_{n,i}) \\ i \neq j & 0 \end{cases}, \quad 1 \leq i, j \leq K \quad (11)$$

From (5), (10) and the definition of  $Z$ , evaluation of

$$E_{\mathbf{h}} \left[ Z^{D_{\mathbf{n}_\beta}^2} | D_{\mathbf{n}_\beta}^2 = d^2(\underline{\mathbf{c}}_K, \underline{\mathbf{e}}_K) \right] = E_{\mathbf{h}} \left[ e^{-\gamma \mathbf{x}^H \mathbf{x}} \right], \quad (12)$$

where  $\gamma = r_c E_b / 4N_0$ . Using [18], we compute the Laplace transform with respect to the quadratic form of a complex Gaussian random variable.

$$E_{\mathbf{h}} \left[ e^{-\gamma \mathbf{x}^H \mathbf{x}} \right] = \det(\mathbf{I}_K + \gamma \mathbf{M}_{\mathbf{x}})^{-1} = \prod_{k=1}^K (1 + \gamma d_k^2)^{-1} \quad (13)$$

where  $\mathbf{I}_K$  is the  $K \times K$  identity matrix. The equivalent SED averaged over fading is

$$\prod_{k=1}^K (1 + \gamma d_k^2)^{-1} = \exp \left( - \sum_{k=1}^K \Delta_k^2 \right) \quad (14)$$

where  $\Delta_k^2 = \log(1 + \gamma d_k^2)$ . The computation of the bound can now proceed as in the AWGN case, with the cumulative SED for a type  $\mathbf{n}_\beta(w, z)$  error sequence being represented by the random variable  $\tilde{D}_{\mathbf{n}_\beta}^2$ , where  $\tilde{D}_{\mathbf{n}_\beta}^2$  has already been averaged over the fading channel. Thus the final expression for the bit error bound is given by

$$P_e \leq \sum_{w=1}^{3K} \sum_{z=0}^{3K} \sum_{\mathbf{n}_\beta(w, z)} \frac{w}{6K} \tilde{a}(6K, w, z) \Phi(w, z, \mathbf{n}_\beta) E \left[ e^{-\tilde{D}_{\mathbf{n}_\beta}^2} \right] \quad (15)$$

### Extension to Multiple Receive Antennas

We now extend the union bound to the case of multiple receive antennas  $M$ .

With the channel matrix  $\mathbf{H}$  in the signal model of (1) consisting of elements  $h_{m,n}$ , the SED in (9) can be rewritten

$$\begin{aligned} \delta^2(\mathbf{c}_k, \mathbf{e}_k) &= \sum_{m=1}^M \left\| \sum_{n=1}^N h_{m,n} (\rho(\mathbf{c}_k^{(n)}) - \rho(\mathbf{c}_k^{(n)} \oplus \mathbf{e}_k^{(n)})) \right\|^2 \\ &= \sum_{m=1}^M \left\| \sum_{n=1}^N h_{m,n} d(c_{n,k}, e_{n,k}) \right\|^2 \end{aligned} \quad (16)$$

It follows that the cumulative SED can be expressed

$$\delta^2(\underline{\mathbf{c}}_K, \underline{\mathbf{e}}_K) = \sum_{k=1}^K \delta^2(\mathbf{c}_k, \mathbf{e}_k) = \bar{\mathbf{x}}^H \bar{\mathbf{x}} \quad (17)$$

The  $MK \times 1$  vector  $\bar{\mathbf{x}}$  is a complex Gaussian multivariate with zero mean and covariance matrix  $\mathbf{M}_{\bar{\mathbf{x}}} = \mathbf{I}_M \otimes \mathbf{M}_{\mathbf{x}}$  where  $\mathbf{M}_{\mathbf{x}}$  was defined in (11),  $\otimes$  is the Kronecker product and  $\mathbf{I}_M$  is the  $M \times M$  identity unity matrix. It follows that similar to (13), we get

$$E_{\mathbf{h}} \left[ e^{-\gamma \bar{\mathbf{x}}^H \bar{\mathbf{x}}} \right] = \det(\mathbf{I}_{MK} + \gamma \mathbf{M}_{\bar{\mathbf{x}}})^{-1} = \prod_{k=1}^K (1 + \gamma \tilde{\Delta}_k^2)^{-M}, \quad (18)$$

resulting in a set of equivalent distances  $\tilde{\Delta}_k^2 = M \log(1 + \gamma d_k^2)$ . Finally a bound similar to (15) is obtained, except that the SED averaged over fading  $\tilde{D}_{\mathbf{n}_\beta}^2$ , incorporates the effect of  $M$  receive antennas.

## V. UNION BOUND EXAMPLES

This part contains numerical examples that demonstrate the union bound derived in section IV. For comparison, simulation results are also provided. The simulation is based on Monte Carlo runs with 10,000 channel realizations for each  $E_b/N_0$ . As in the numerical examples of Section III, the channel model was Rayleigh block-fading, meaning that the channel was assumed constant during a frame of  $F = 130$  symbols, but independent frame-to-frame. Simulation results shown are averaged over random interleavers of size as specified in the figures. The union bound is found for 16 state 8-PSK turbo-STCM with constituent codes shown in Fig. 1.

Fig. 9 and 10 respectively, provide the performance analysis for single and two receive antennas. Simulations results are shown after eight iterations of the turbo decoder. Each figure is divided in two parts corresponding to interleaver sizes  $K = 1300$  and  $5200$  symbols, respectively. The expression specifies a bound obtained by summing over all error sequences with systematic weights  $1 \leq w \leq 3K$ , and parity weights  $0 \leq z \leq 3K$ . Computation of the full bound is prohibitive in its complexity and it is also unnecessary. One of the analysis goals is to investigate how many terms are required to obtain a good approximation of the union bound. Each curve in each figure is labeled with the weights  $w$  of the error sequences. In all cases, the parity terms included in the bound were

$0 \leq z \leq 15$ . The justification of using a small subset of error sequences is that the small weights result in sequences with small SED's, which in turn, contribute the dominant terms to the union bound. From the figures it can be observed that error sequences corresponding to  $w = 2$  are sufficient to provide a good approximation to the error bound. For example, it can be observed from Fig. 9 (b) that the curves for  $w \geq 2$  coalesce for  $E_b/N_0 \geq 20$  dB. Similarly, for the two receive antenna case, in Fig. 10 (b) the curves coalesce for  $E_b/N_0 \geq 14$  dB. These results justify simplifying the bound evaluation by neglecting terms with large weights.

## VI. CONCLUSION

In this paper we analyzed a turbo coding scheme, referred to as turbo-STCM, featuring space-time constituent codes. The scheme provides full diversity and full rate. Performance over a flat block-fading Rayleigh channel is demonstrated by simulations for 3 bits/s/Hz 16 state 8-PSK turbo-STCM codes. Turbo-STCM with a fixed interleaver has an performance improvement over 64 state Tarokh code of 2.3 dB after 8 iterations for the two transmit-one receive antenna configuration at FER =  $10^{-1}$ .

The analytical union bound is derived for 3 bits/s/Hz, 8-PSK turbo-STCM with two transmit-one/two receive antennas over the block-fading Rayleigh channel. The union bound is expressed in terms of the input output weight enumerators of the constituent codes, the interleaver size, and the spectrum of the squared Euclidean distance spectrum. It is shown that a small number of terms with low systematic bit weights is sufficient to yield an accurate upper bound on the bit error. In conclusion to the work presented in this paper, turbo-STCM codes have the potential to facilitate high-rate data transmission over fading channels in future wireless networks. The analysis developed in the paper provides a practical tool to analyze the performance of these turbo codes.

## REFERENCES

- [1] C. Berrou, A. Glavieux, and P. Thititmajshima, "Near Shannon limit error-correcting coding and decoding: Turbo-codes (1)," *IEEE International Conference on Communications (ICC '93)*, pp. 1064–1070, May 1993.
- [2] V. Tarokh, N. Seshadri and A.R. Calderbank, "Space-time codes for high data rate wireless communications: Performance criterion and code construction," *IEEE Transactions on Information Theory*, vol. 44, pp. 744–765, Mar. 1998.
- [3] S. Baro, G. Bauch, and A. Hansmann, "Improved codes for space-time trellis-coded modulation," *IEEE Communications Letters*, vol. 4, pp. 20–22, Jan. 2000.
- [4] X. Lin and R.S. Blum, "Improved space-time codes using serial concatenation," *IEEE Communications Letters*, vol. 4, pp. 221–223, Jul. 2000.
- [5] K.R. Narayanan, "Turbo decoding of concatenated space-time codes," *37th Annual Allerton Conference on Communication, Control and Computing*, Sept. 1999.
- [6] A. Stefanov and T.M. Duman, "Turbo coded modulation for wireless communications with antenna diversity," *IEEE VTC '99*, pp. 1565–1569, 1999.
- [7] H. Su and E. Geraniotis, "Spectrally efficient Turbo codes with full antenna diversity," *Multiaccess Mobility and Teletraffic for Wireless Communications (MMT '99)*, Oct. 1999.

- [8] Y. Liu and M.P. Fitz, "Space-time turbo codes," *37th Annual Allerton Conference on Communication, Control and Computing*, Sept. 1999.
- [9] P. Robertson and T. Wörz, "Bandwidth-efficient turbo trellis-coded modulation using punctured component codes," *IEEE Journal on Selected Areas in Communications*, vol. 16, pp. 206–218, Feb. 1998.
- [10] D. Cui and A.M. Haimovich, "A new bandwidth efficient antenna diversity scheme using turbo codes," *34th Annual Conference on Information Sciences and Systems (CISS '00)*, vol. 1, pp. TA-6.24–29, Mar. 2000, Princeton, NJ.
- [11] D. Cui and A.M. Haimovich, "Design and performance analysis of turbo space-time coded modulation," *IEEE Global Telecommunications conference (Globecom '00)*, vol. 3, pp. 1627–1631, Nov. 27–Dec. 1 2000, San Francisco, CA.
- [12] D. Cui and A.M. Haimovich, "Performance of parallel concatenated space-time codes," *Accepted by IEEE Communications Letter*, Jan. 2001.
- [13] D. Cui and A.M. Haimovich, "Error performance analysis of turbo space-time coded modulation over fading channels," *IEEE International Conference on Communications (ICC '01)*, Jun. 2001, Helsinki, Finland.
- [14] L.R. Bahl, J. Cocke, F. Jelinek, and J. Raviv, "Optimal decoding of linear codes for minimizing symbol error rate," *IEEE Transactions on Information Theory*, pp. 284–287, Mar. 1974.
- [15] D. Divsalar and F. Pollara, "Turbo codes for PCS applications," *IEEE International Conference on Communications (ICC '95)*, vol. 1, pp. 54–59, 1995.
- [16] M.C. Valenti, *Iterative Detection and Decoding for Wireless Communication*, Ph.D. thesis, Electrical Engineering Department, Virginia Polytechnic Institute and State University, Blacksburg, Virginia., Jul. 1999.
- [17] Dongzhe Cui, *Turbo Space-Time Coded Modulation: Principles and Performance Analysis*, Ph.D. thesis, Electrical and Computer Engineering Department, New Jersey Institute of Technology, Newark, New Jersey, May. 2001.
- [18] G.L. Turin, "The characteristic function of hermitian quadratic forms in complex normal variables," *Biometrika*, vol. 47, pp. 199–212, Jun. 1960.

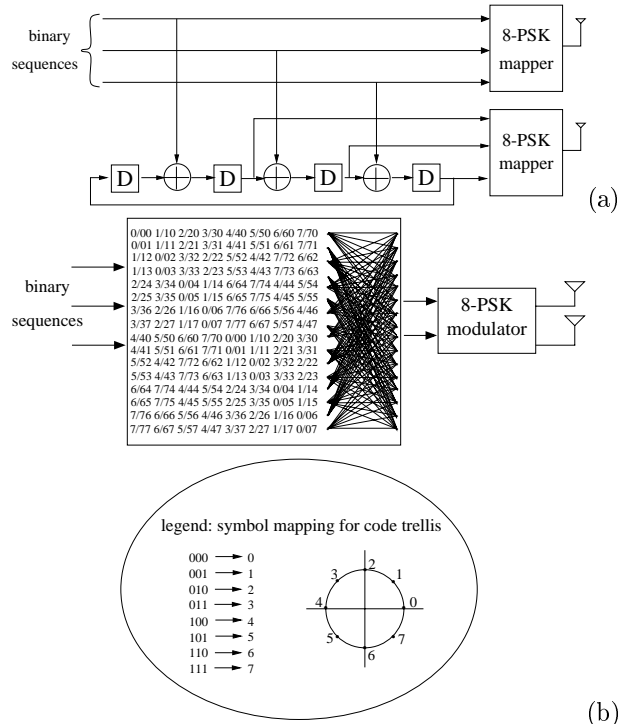


Fig. 1. Recursive systematic space-time encoder for 16-state 8-PSK, 2 transmit antennas, 3 bits/s/Hz. (a) code implementation, (b) code trellis

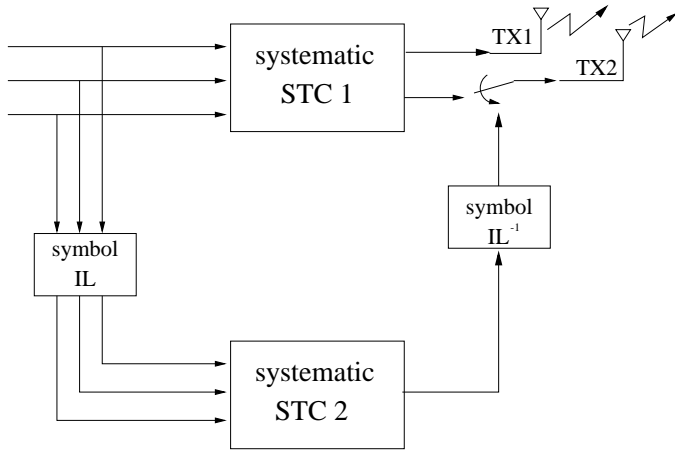


Fig. 2. Turbo-STCM encoder, 2 transmit antennas, 3 bits/s/Hz.

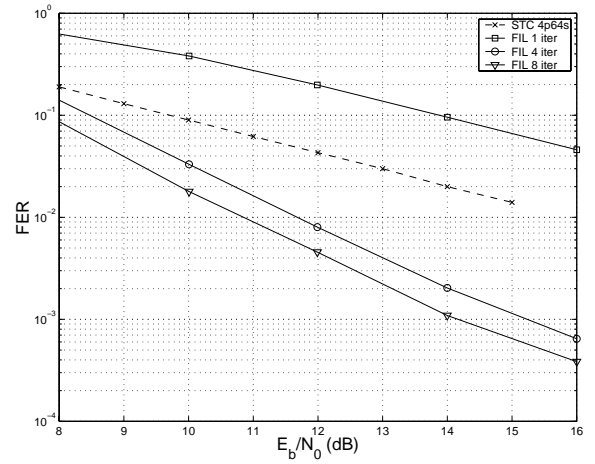


Fig. 5. FER of turbo-STCM 8 state 4-PSK over fading channel, with recursive terminated space-time component code and fixed interleaver (FIL) of size  $K = 1300$  symbols.

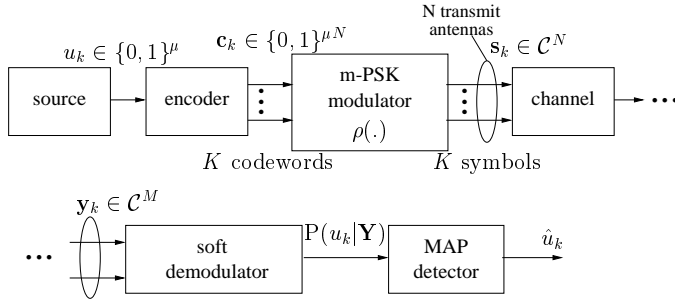


Fig. 3. Schematic diagram of transmission system.

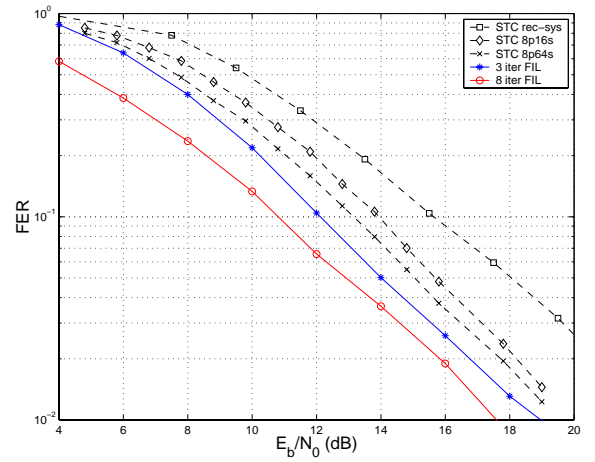


Fig. 6. FER of turbo-STCM (2T1R) 16 state 8-PSK over fading channel, with fixed interleaver (FIL) of size  $K = 1300$  symbols.

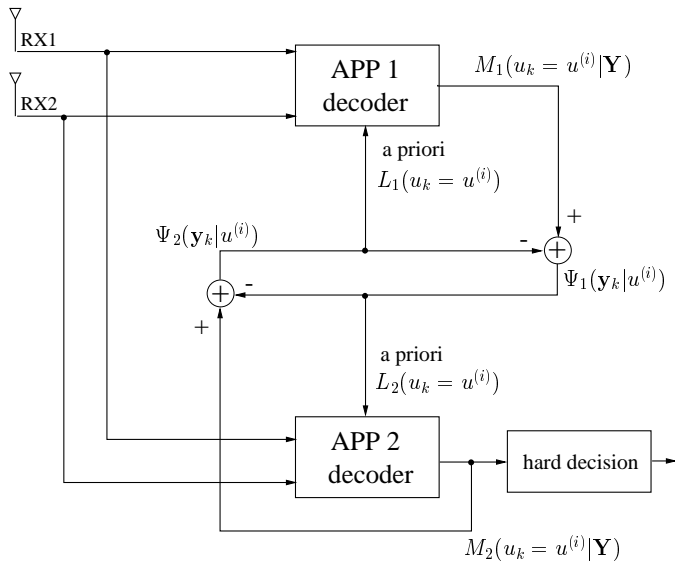


Fig. 4. Turbo-STCM decoder, the interleavers/deinterleavers are not shown.

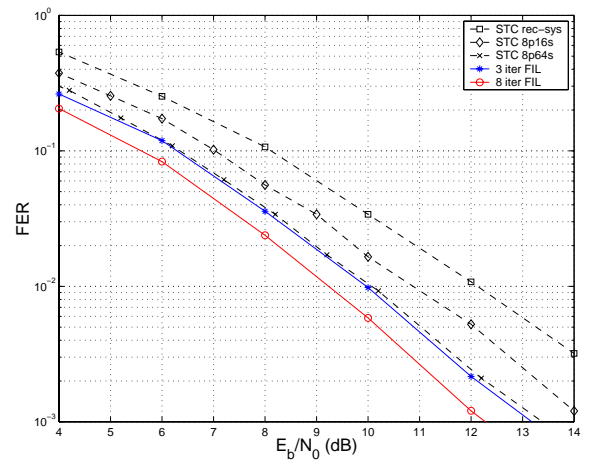


Fig. 7. FER of turbo-STCM (2T2R) 16 state 8-PSK over fading channel, with fixed interleaver (FIL) of size  $K = 1300$  symbols.

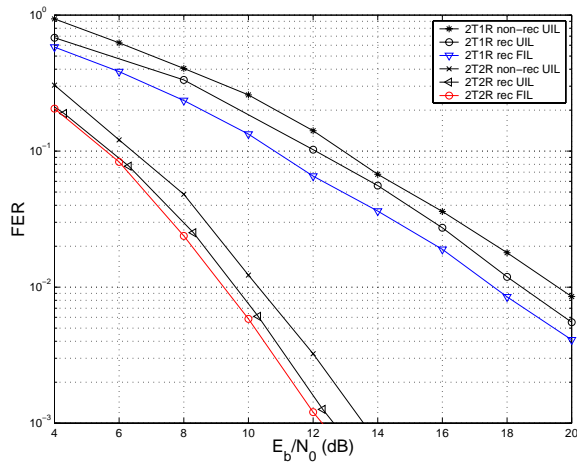
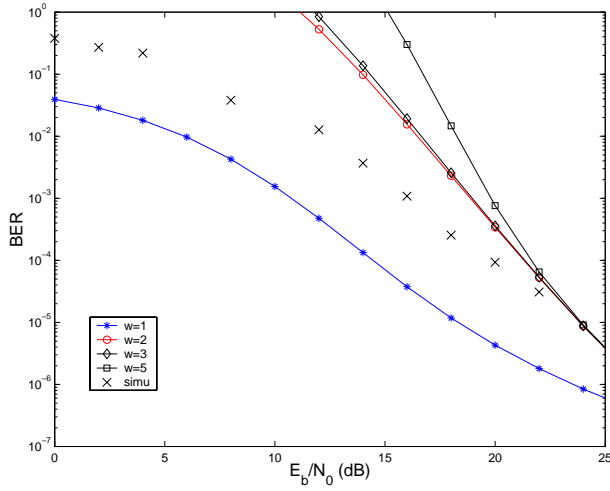
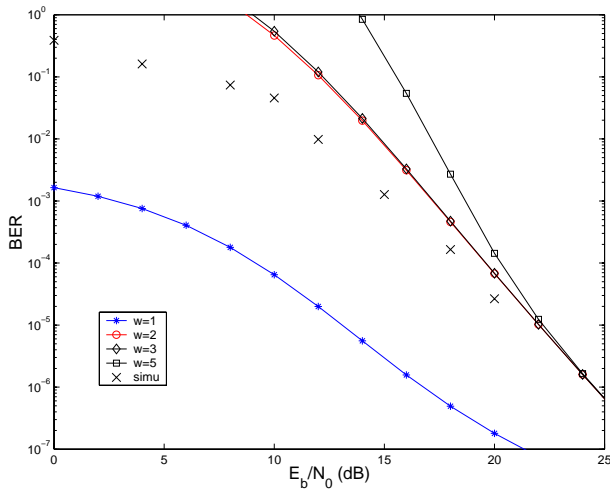


Fig. 8. FER comparison of turbo-STCM 16 state 8-PSK over fading channel, with recursive and non-recursive STC, fixed interleaver (FIL) and averaged over interleavers (UIL).

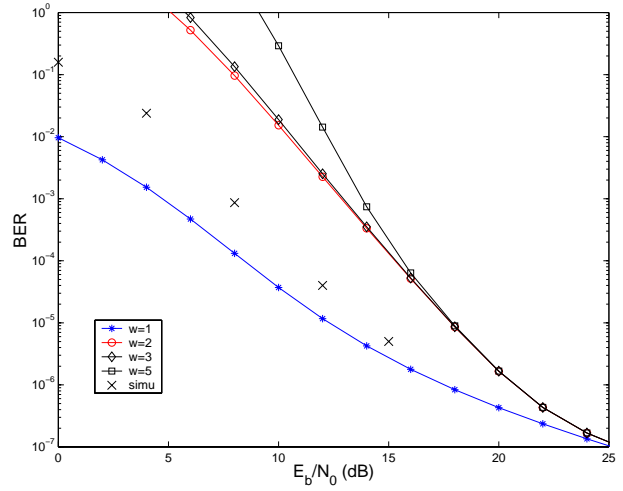


(a)

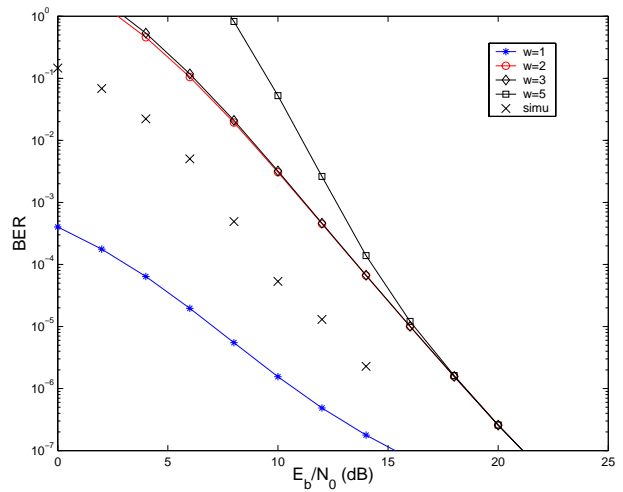


(b)

Fig. 9. Union bound for turbo-STCM (2T1R) over block-fading channel with block length (symbols): (a)  $K = 1300$ , (b)  $K = 5200$ .



(a)



(b)

Fig. 10. Union bound for turbo-STCM (2T2R) over block-fading channel with block length (symbols): (a)  $K = 1300$ , (b)  $K = 5200$ .